

# Supercurrent through Hybrid Junctions with Anisotropic Cooper-Pair Condensates

Munehiro Nishida,<sup>1,2</sup> Noriyuki Hatakenaka,<sup>1,3</sup> and Susumu Kurihara<sup>2</sup>

<sup>1</sup>*Low Temperature Laboratory, Helsinki University of Technology, P.O. Box 2200 FIN-02015 HUT, Finland*

<sup>2</sup>*Department of Physics, Waseda University, Okubo, Shinjuku-ku, Tokyo 169-8555 Japan*

<sup>3</sup>*NTT Basic Research Laboratories, Atsugi, Kanagawa 243-0198, Japan*

(Received 23 August 2001; published 26 March 2002)

A general formula for the supercurrent between different internal structures in a wide class of hybrid junctions is derived on the basis of the Andreev-reflection picture. The formula extends existing formulas and also enables us to analyze novel *B*-phase/*A*-phase/*B*-phase junctions in superfluid <sup>3</sup>He systems. We propose a mechanism for  $\pi$  states due to the  $\hat{l}$  texture in the *A* phase of the junction, which could elucidate major features of the  $\pi$  states with higher critical current (**H** states) discovered in superfluid <sup>3</sup>He weak links. The bistability of the  $\pi$  states is also discussed.

DOI: 10.1103/PhysRevLett.88.145302

PACS numbers: 67.57.Fg, 74.50.+r, 74.80.Fp

Superfluid systems with internal degrees of freedom produce diverse ordered structures, which provide a new arena for exploring the fertile physics behind them. The Josephson effect [1] extracts the global phase resulting from the spontaneous breakdown of gauge symmetry. Moreover, it also exposes the internal structures formed from other broken symmetries. In fact, so-called  $\pi$  junctions associated with high- $T_c$  superconductors provide convincing evidence for *d*-wave symmetry [2,3], and recent experiments on Pb-Sr<sub>2</sub>RuO<sub>4</sub>-Pb Josephson junctions [4] could be explained by *p*-wave superconductivity in Sr<sub>2</sub>RuO<sub>4</sub> [5,6]. In addition, metastable  $\pi$  states observed in superfluid <sup>3</sup>He weak links [7–9] are considered to be a signature of texture due to the internal degrees of freedom of *p*-wave order parameters [10–12], but the mechanism for the  $\pi$  states remains unsettled. In this Letter, we derive a general formula for supercurrent, applicable to a wide class of hybrid junctions between different internal structures in unitary states, on the basis of the Andreev-reflection (AR) picture developed by Furusaki and Tsukada (FT) [13], and then apply it to a novel hybrid junction consisting of *B*-phase/*A*-phase/*B*-phase in superfluid <sup>3</sup>He systems giving an alternative explanation of the  $\pi$  states.

The Andreev reflection is a unique quantum scattering process which occurs at the boundary between condensates: an injected particlelike quasiparticle (PLQ) to the interface is reflected back by the pair potential as a holelike quasiparticle (HLQ) and vice versa [14]. The supercurrent through junctions can be considered as a series of the Andreev reflection at two interfaces. A Cooper pair breaks into two quasiparticles at one interface, namely one outgoing PLQ and one incoming HLQ. The quasiparticles propagate to the other interface and thus combine to form a Cooper pair. The pair is then transferred from one side to the other. Therefore, the supercurrent is written by means of scattering coefficients related to the Andreev reflection.

Consider a junction composed of  $N + 2$  different superfluid regions separated with flat interfaces perpendicular to the  $z$  axis. The interfaces are located at  $z = z_i$  ( $i = 0, 1, 2, \dots, N$ ) with  $z_0 = 0$  and  $z_N = L$ . We shall denote

these regions by  $L$  ( $= C_0, z < 0$ ),  $C_i$  ( $z_{i-1} < z < z_i, i = 1, \dots, N$ ), and  $R$  ( $= C_{N+1}, L < z$ ), respectively. We assume that the order parameter is uniform in each region. We also assume that the effective mass  $m$ , Fermi velocity  $v_F$ , and Fermi wave number  $k_F$  are the same in all regions. The potential barriers at the interfaces are ignored for simplicity. We shall use a triad ( $\hat{x}, \hat{y}, \hat{z}$ ) for a frame of reference.

The AR coefficients are obtained by solving the Bogoliubov–de Gennes equations which can be reduced to the Andreev equations in a quasiclassical approximation [14]. The Andreev equations for an arbitrary type of pairing [15] are

$$\begin{bmatrix} (-i\hbar v_F \hat{k}_z \frac{\partial}{\partial z} - E)\hat{1} & \hat{\Delta}^{\hat{k}} \\ \hat{\Delta}^{\hat{k}\dagger} & (i\hbar v_F \hat{k}_z \frac{\partial}{\partial z} - E)\hat{1} \end{bmatrix} \begin{pmatrix} u \\ v \end{pmatrix} = 0, \quad (1)$$

where  $u = (u_\uparrow u_\downarrow)^t$  and  $v = (v_\uparrow v_\downarrow)^t$  with  $u_\sigma$  and  $v_\sigma$  being the wave function for a particle and a hole with spin  $\sigma$ , respectively.  $\hat{1}$  is the  $2 \times 2$  unit matrix and  $E$  is the energy of a quasiparticle. The direction of the quasiparticle momentum and the gap matrix in spin space are denoted by a unit vector  $\hat{k} = (\hat{k}_x, \hat{k}_y, \hat{k}_z)$  and  $\hat{\Delta}^{\hat{k}}$ , respectively. In each region  $C_i$ , the gap matrix  $\hat{\Delta}_i^{\hat{k}}$  is assumed to be constant and unitary:  $\hat{\Delta}_i^{\hat{k}} \cdot \hat{\Delta}_i^{\hat{k}\dagger} = |\Delta_i^{\hat{k}}|^2 \hat{1}$ .

The solutions of Andreev equations for each region  $C_i$  can be constructed by a linear combination of wave functions of PLQ  $\propto e^{i\nu_i^{\hat{k}} z}$  and HLQ  $\propto e^{-i\nu_i^{\hat{k}} z}$  with  $\nu_i^{\hat{k}} = \Omega_i^{\hat{k}} / \hbar v_F \hat{k}_z$  and  $\Omega_i^{\hat{k}} = \sqrt{E^2 - |\Delta_i^{\hat{k}}|^2}$ , and are given as

$$\begin{pmatrix} u^i \\ v^i \end{pmatrix} = \begin{bmatrix} (E + \Omega_i^{\hat{k}})\hat{1}e^{i\nu_i^{\hat{k}} z} & \hat{\Delta}_i^{\hat{k}} e^{-i\nu_i^{\hat{k}} z} \\ \hat{\Delta}_i^{\hat{k}\dagger} e^{i\nu_i^{\hat{k}} z} & (E + \Omega_i^{\hat{k}})\hat{1}e^{-i\nu_i^{\hat{k}} z} \end{bmatrix} \begin{pmatrix} p_\sigma^i \\ h_\sigma^i \end{pmatrix} \equiv M_i^{\hat{k}}(z) \begin{pmatrix} p_\sigma^i \\ h_\sigma^i \end{pmatrix}, \quad (2)$$

where  $p_\sigma^i = (p_{\uparrow\sigma}^i p_{\downarrow\sigma}^i)^t$  and  $h_\sigma^i = (h_{\uparrow\sigma}^i h_{\downarrow\sigma}^i)^t$  with  $p_{\sigma\sigma'}^i$

(or  $h_{\sigma\sigma'}$ ) being the scattering coefficient in which an injected quasiparticle with spin  $\sigma'$  is scattered as a PLQ (or HLQ) with spin  $\sigma$ . Figure 1 shows the AR processes where a PLQ is injected with different spin, i.e., (a) up-spin and (b) down-spin. By introducing scattering coefficient matrices  $\hat{p}^i = (p_{\sigma\sigma'}^i)$  and  $\hat{h}^i = (h_{\sigma\sigma'}^i)$ , these two processes can be treated as a single process. The AR coefficient matrix is given by  $\hat{a} = \hat{h}^0$ . The coefficients  $\hat{S}^i = (\hat{p}^i \hat{h}^i)^t$  are connected by the continuity condition for the wave function:  $M_i^{\hat{k}}(z_i) \hat{S}^i = M_{i+1}^{\hat{k}}(z_i) \hat{S}^{i+1}$ , namely,  $\hat{S}^i = M_i^{\hat{k}}(z_i)^{-1} M_{i+1}^{\hat{k}}(z_i) \hat{S}^{i+1} \equiv T_i \hat{S}^{i+1}$ . For a whole system, we obtain

$$\begin{pmatrix} \hat{1} \\ \hat{a} \end{pmatrix} = \prod_{i=0}^N T_i \begin{pmatrix} \hat{b} \\ \hat{0} \end{pmatrix} \equiv \begin{pmatrix} \hat{T}_{pp} & \hat{T}_{ph} \\ \hat{T}_{hp} & \hat{T}_{hh} \end{pmatrix} \begin{pmatrix} \hat{b} \\ \hat{0} \end{pmatrix}, \quad (3)$$

where  $\hat{0}$  is the  $2 \times 2$  zero matrix and  $\{\hat{T}_{qq'}\}$  are each  $2 \times 2$  parts of the  $4 \times 4$  transfer matrix from R to L. Therefore, the AR coefficient matrix  $\hat{a}$  is obtained as

$$\hat{a} = \hat{T}_{hp} \hat{T}_{pp}^{-1}. \quad (4)$$

$$\mathcal{G}(z, z', \mathbf{k}_{\parallel}, \omega_n) = i \frac{m}{\hbar^2 k_F \hat{k}_z} \times \left[ \frac{e^{-ik_F \hat{k}_z(z-z')} \tilde{\mathbf{M}}_0^{\hat{k}_-}(z) \begin{pmatrix} \hat{1} \\ \hat{0} \end{pmatrix} \begin{pmatrix} \hat{0} \\ \hat{a} \end{pmatrix} \tilde{\mathbf{M}}_0^{\hat{k}_-}(z')^\dagger}{(\omega_n + \tilde{\Omega}_0^{\hat{k}_-})^2 + |\Delta_0^{\hat{k}_-}|^2} + \frac{e^{ik_F \hat{k}_z(z-z')} \tilde{\mathbf{M}}_0^{\hat{k}}(z) \begin{pmatrix} \hat{0} \\ \hat{a} \end{pmatrix} \tilde{\mathbf{M}}_0^{\hat{k}}(z')^\dagger}{(\omega_n + \tilde{\Omega}_0^{\hat{k}})^2 + |\Delta_0^{\hat{k}}|^2} \right], \quad (5)$$

where  $\hat{k}_- = \mathbf{k}_{\parallel}/k_F - \hat{k}_z \hat{z}$  and  $\tilde{\mathbf{M}}_0^{\hat{k}}$  is obtained by an analytic continuation  $E \rightarrow i\omega_n$  from  $\mathbf{M}_0^{\hat{k}}$ . The matrix  $\tilde{\mathbf{a}}$  describes the reverse process in which a HLQ injected from L is reflected as a PLQ. The matrices  $\tilde{\mathbf{a}}$  and  $\hat{\mathbf{a}}$  are related by  $\tilde{\mathbf{a}}(E, \hat{\mathbf{k}}) = \hat{\mathbf{a}}(E, \hat{\mathbf{k}}_-)^\dagger$ .

A general formula for the supercurrent through weak links at temperature  $T$  per unit area is derived as

$$I = - \int \frac{d^2 k_{\parallel}}{8\pi^2 \hbar \beta} \sum_{\omega_n} \text{Tr} \left[ \frac{\hat{\Delta}_0^{\hat{k}} \hat{\mathbf{a}}(\omega_n)}{\tilde{\Omega}_0^{\hat{k}}} - \frac{\tilde{\mathbf{a}}(\omega_n) \hat{\Delta}_0^{\hat{k}_-}}{\tilde{\Omega}_0^{\hat{k}_-}} \right], \quad (6)$$

where  $\tilde{\Omega}_0^{\hat{k}} = \sqrt{\omega_n^2 + |\Delta_0^{\hat{k}}|^2}$ . This is the central result of this Letter. This formula is applicable to any type of hybrid junctions between unitary states with any symmetry. Note that our formula still preserves the original FT form expressed by the difference between AR coefficients, describing the net current carried by the two processes: the scattering of a PLQ into a HLQ and its reverse process. Our formula covers the previous formulas, for example the Kurkijärvi formula [16] for superfluid  $^3\text{He}$  systems, the Tanaka-Kashiwaya formula [17] for unconventional *singlet* superconductors and so on [5,18,19], by taking appropriate conditions such as  $L \rightarrow 0$  and/or  $\Delta_{Ci} \rightarrow 0$ .

Our formula also enables us to analyze new kinds of junctions. One example is *B-phase/A-phase/B-phase* (BAB) junctions in superfluid  $^3\text{He}$  systems, which could be realized by using the experimental setup for the

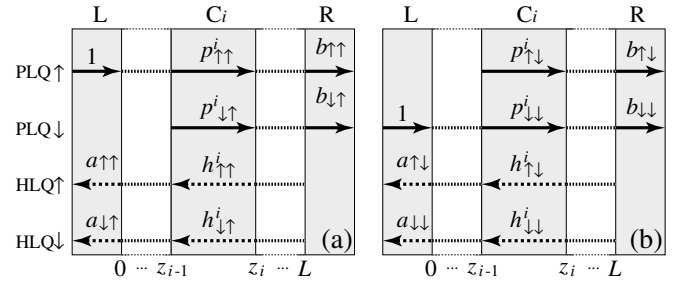


FIG. 1. (a) The AR process in which a PLQ with *up spin* is injected from the region L reflected as a HLQ. The solid and dashed arrows denote PLQ and HLQ propagations, respectively. The symbols on the arrows are the scattering coefficients. (b) The process in which a PLQ with *down spin* is injected.

The currents are calculated from the wave functions with the AR coefficients. At finite temperatures  $T$ , the current is evaluated by statistical averaging with the help of the temperature Green's function,  $\mathcal{G}(z, z', \mathbf{k}_{\parallel}, \omega_n)$ , where  $\omega_n = \pi(2n + 1)/\beta$  ( $n = 0, \pm 1, \pm 2, \dots$ ) with  $\beta = 1/k_B T$ , and  $\mathbf{k}_{\parallel} \equiv k_F(\hat{k}_x, \hat{k}_y, 0)$  is the momentum in the *xy* plane. The temperature Green's function is constructed from the scattering coefficient matrices under the FT prescriptions [13]. For  $z \leq z' < 0$ , the temperature Green's function is given by

Andreev reflection at AB interfaces [20]. Here we introduce a wall with a pinhole in the A-phase region as shown in Fig. 2, in order to imitate the Berkeley's system and to produce appreciable phase drops across the junction [21]. Therefore, this system contains four different superfluid regions.

According to the AR picture, the current is greatly influenced by the structure of order parameter. In *spin-triplet p-wave* condensates, ordered structures (textures) are formed by spontaneously broken spin-orbit symmetry. The order parameter of the A phase is defined by a triad  $(\hat{\mathbf{w}}_1, \hat{\mathbf{w}}_2, \hat{\mathbf{l}})$  in orbital space and a vector  $\hat{\mathbf{d}}$  in spin space. For the B phase we need a rotational matrix  $R(\hat{\mathbf{n}}, \theta)$  with rotational axis  $\hat{\mathbf{n}}$  and rotational angle  $\theta$  relating the spin space to the orbital space. Therefore, special attention should

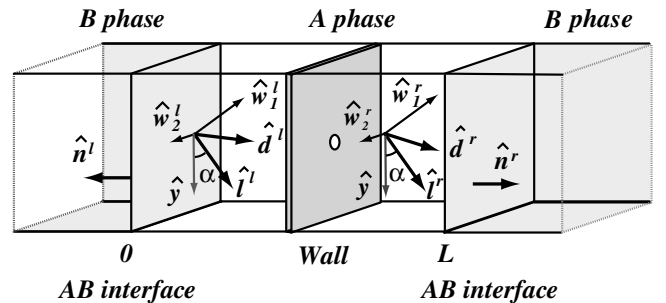


FIG. 2. Schematic diagram of a BAB junction.

be paid to  $\hat{l}$  in the  $A$  phase and to  $\hat{n}$  in the  $B$  phase. Indeed, for  $^3\text{He-B}$  weak links, the  $\hat{n}$  vector determines the current-phase relations [10–12]. While for  $^3\text{He-A}$  weak links, the striking effect has been predicted [16,22] that no supercurrent can flow if the  $\hat{l}$  vectors between the link are antiparallel.

The boundary conditions at  $AB$  interfaces is determined by minimizing the surface energy [23–25]. Here we consider the dipole-dipole interaction only in the  $B$  phase since the width of the  $A$ -phase layer is assumed to be less than the dipole coherence length. There are two boundary conditions (i)  $\hat{d} = R(\hat{n}, \theta_L)\hat{w}_1$  and (ii)  $\hat{w}_1 \parallel \hat{z}$  (therefore  $\hat{l} \perp \hat{z}$ ), where  $\theta_L = \cos^{-1}(-1/4)$  (Leggett angle). We assume that the condition (i) is always satisfied from energy considerations. The texture of  $A$  phase should be formed so as to satisfy boundary conditions at both  $AB$  interfaces and the wall. To gain condensation energies, the  $\hat{l}$  vector tends to orient perpendicular to the wall, while parallel to the  $AB$  boundary. Because of the competition between them,  $\hat{l}$  is likely to lean considerably from the wall without bending if  $A$ -phase layer is thin. Thus we assume that the  $\hat{l}$  vectors in both sides of the  $A$  phases tilt from the  $y$  axis by the angle  $\alpha$  in the  $yz$  plane. We also assume the  $\hat{n}$  vectors in the  $B$  phases are antiparallel for a later convenience since actual configurations depend on experimental geometries [12].

To unearth the role of the  $A$  phase in the  $BAB$  junction, we investigate the effect of  $\hat{l}$  textures on current-phase relations. Figure 3(a) shows current-phase relations with different  $\hat{l}$ -vector orientations at  $T = 0.1T_c$ . Here, the width of the  $A$ -phase region  $L$  is  $6\xi_0$  where the coherence length  $\xi_0$  in the  $B$  phase at zero temperature is given by  $\xi_0 = [7\zeta(3)/48]^{1/2}(\hbar v_F/\pi k_B T_c)$  with  $\zeta$  being the Riemann zeta function. We observe  $\pi$  states on current-phase relations around  $\alpha = 0.2\pi \sim 0.35\pi$ . The  $\pi$  states in  $^3\text{He-B}$  are due to the cancellations of currents carried by quasiparticles with different spins which acquire different excess phases from the internal spin structure of the order parameter while travelling through the system (the  $\hat{n}$ -texture mechanism). The  $\pi$  states in Fig. 3(a) are

quite different from those of the  $\hat{n}$ -texture mechanism (the dotted curve) in shape as well as magnitude of the current. This infers that quasiparticles acquire the excess phase in the  $A$  phase in addition to the  $B$  phase.

Figure 3(b) shows current-phase relations with different widths  $L$ . Clearly the relation reduces to that of  $^3\text{He-B}$  weak links as  $L \rightarrow 0$ . The relations change drastically in their shape and magnitude from the relation of zero width as  $L$  increases. In particular, the current suddenly drops when the phase difference exceeds the value at the maximum current. We confirm that the current in the large  $L$  limit is identical to that of  $^3\text{He-A}$  weak links. As a result, the  $\pi$  states can form due to excess phase acquired from the texture in  $A$  phase. In the intermediate widths, both  $\hat{l}$  and  $\hat{n}$  characteristics are intermingled.

Let us discuss the mechanism for  $\pi$  states due to the  $\hat{l}$  texture in the  $A$  phase. The  $\hat{d}$  vector in the  $A$  phase changes its direction through the first  $AB$  boundary condition (i) when the  $\hat{l}$  vector tilts from the interface. Since the  $\hat{n}$  vectors in each  $B$  phase are antiparallel, the  $\hat{d}$  vectors orient two different directions,  $\hat{d}^l$  and  $\hat{d}^r$ . In this case, quasiparticles with different spins, namely *up spin* and *down spin*, see the different phases while traveling through the  $A$  phase. It will be clear if we take a spin-quantization axis as  $\hat{d}^l \times \hat{d}^r$ . The gap matrices are diagonalized as

$$\hat{\Delta}_l^k \propto \begin{pmatrix} -e^{-i\phi^l} & 0 \\ 0 & e^{i\phi^l} \end{pmatrix}, \quad \hat{\Delta}_r^k \propto \begin{pmatrix} -e^{-i\phi^r} & 0 \\ 0 & e^{i\phi^r} \end{pmatrix}, \quad (7)$$

where  $\phi^i$  ( $i = r$  or  $l$ ) is the azimuthal angle of  $\hat{d}^i$  in the plane perpendicular to  $\hat{d}^l \times \hat{d}^r$ . Quasiparticles acquire the excess phase  $\phi^r - \phi^l$ , namely, the relative angle between  $\hat{d}^l$  and  $\hat{d}^r$ . This excess phase modifies the current-phase relations, and results in the  $\pi$  states due to the current cancellations in spin space (the  $\hat{l}$ -texture mechanism). An essential difference from the  $\hat{n}$ -texture mechanism [10] is that the excess phase  $\phi^i$  has no  $\mathbf{k}$  dependence in  $A$  phase, keeping the current cancellation intact. This makes  $\pi$  states pronounced and suppresses the critical current reduction. Note that there are no mechanisms to fix the

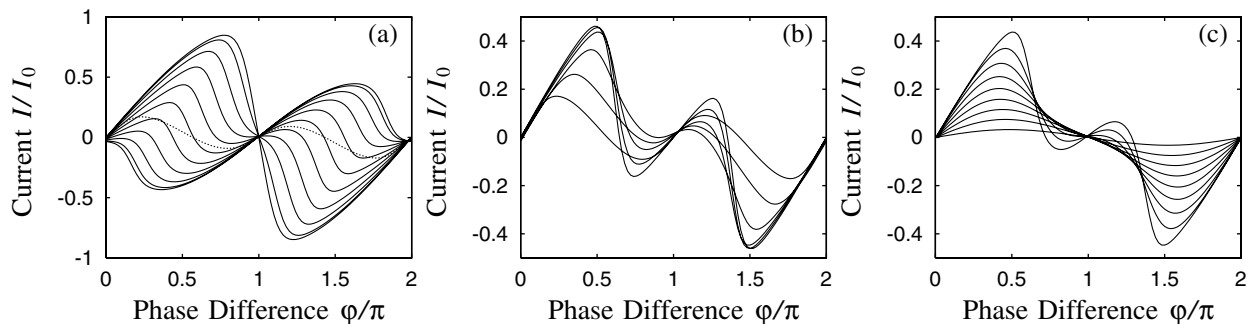


FIG. 3. The current-phase relations of  $BAB$  junctions. (a)  $\alpha$  dependence:  $\alpha = 0 \sim 0.5\pi$  with the step of  $0.05\pi$  in decreasing order of gradient at the origin.  $L = 6\xi_0$  and  $T = 0.1T_c$ . The dotted line denotes the current for  $L = 0$ , namely,  $BB$  junctions. (b)  $L$  dependence:  $L = 0, 0.6\xi_0, 2\xi_0, 6\xi_0, 10\xi_0$ , and  $\infty$  in increasing order of critical current.  $T = 0.1T_c$  and  $\alpha = 0.2\pi$ . (c)  $T$  dependence:  $T = 0.1T_c \sim 0.9T_c$  with the step of  $0.1T_c$  in decreasing order of critical current.  $\alpha = 0.2\pi$  and  $L = 6\xi_0$ . Here,  $I_0 = \Delta_B k_F^2 / 4\pi\hbar \sim 1 \times 10^{23} / \text{cm}^2 \text{ s}$ .

$\hat{d}$  vectors with different directions in  $A$  phases themselves so that specific mechanisms, i.e., the  $AB$  interfaces, are required for  $\pi$  state formation in  $^3\text{He}$ - $A$  weak links.

In experiments [8], the two distinct  $\pi$  states with different critical currents called  $\mathbf{L}$  and  $\mathbf{H}$  states, which depends on detailed cooldown procedure, are observed; “Rapid cooling through  $T_c$  and high levels of acoustic noise in the cell at the time of the superfluid transition favor the  $\mathbf{L}$  state over  $\mathbf{H}$ .” The existing theories based on the  $\hat{n}$ -texture mechanism [10–12], however, seem insufficient to explain both states at the same time. Successive experiment strongly suggests that a pseudo- $A$  phase could be formed around the orifice in  $^3\text{He}$  weak links [26]. The pseudo- $A$  phase formation near the surface has been also predicted [27]. These support our proposal of the  $BAB$  junction as a possible model for the experiment.

Figure 3(c) shows the temperature dependence of current-phase relations under  $\alpha = 0.2\pi$  and  $L = 6\xi_0$  indicating  $\hat{l}$ -texture character. The current-phase relations possess the major characteristics of the  $\mathbf{H}$  state; (1) the phase at maximum current is over  $0.5\pi$ , (2) the current steeply drops after maximum current (*slanted* sine curve), and (3) the magnitude of critical current (e.g.,  $0.2I_0$  at  $T = 0.5T_c$ , which corresponds to a mass current of  $\sim 4 \times 10^{-8}$  g/sec) is in reasonable agreement with the current in experiment. Thus the  $\hat{l}$ -texture mechanism could elucidate major features of the  $\mathbf{H}$  states. On the other hand, under the noisy background, the  $A$ -phase layer near the wall might be difficult to establish. A dominant mechanism to the current is due to the  $\hat{n}$ -texture mechanism, resulting in the  $\mathbf{L}$  states. Therefore, the bistability of the  $\pi$  states would originate from different textures ( $\hat{l}$  or  $\hat{n}$ ) depending on the existence of the pseudo- $A$  phase near the wall.

We have assumed flat interfaces without thickness even though order parameters need to change on the scale of the coherence length. However, qualitative features of our results would be unchanged in spite of our simplified model since only asymptotic behaviors are relevant in scattering theory. Self-consistent calculations taking into account spatial dependence and phase-difference dependence (*anisotextural effect* [11,12]) of order parameter might be needed for quantitative discussions.

In summary, we have derived a general formula for supercurrent through any type of hybrid junctions between unitary states with any symmetry and applied to novel  $BAB$  junctions in superfluid  $^3\text{He}$ . We have proposed the  $\pi$ -state formation mechanism due to  $\hat{l}$  textures in the  $A$  phase. The bistability of the  $\pi$  states could be explained by two different ( $\hat{l}$  or  $\hat{n}$ ) textures in superfluid  $^3\text{He}$  systems.

We thank E. V. Thuneberg, J. Viljas, G. E. Volovik, M. Krusius, L. Skrvák, J. Kopu, D. Meacock, and A. J. Leggett for stimulating discussions. We are grateful to Y. Tanaka, Y. Ohashi, and K. Shirahama for valuable

input. We also thank Y. Asano for sending us his preprint. N.H. is indebted to H. Takayanagi and M. Paalanen for their continuous encouragement. This work was supported in part by the Waseda University Grant for Special Research Projects (2000A-875), by the COE Program “Molecular Nano-Engineering” from the Ministry of Education, Science and Culture, Japan, and by the Helsinki University of Technology and the National Technology Agency Tekes.

*Note added.*—During the preparation of this Letter, we learned of a theory [28] related to Josephson current in a similar system.

- 
- [1] B. D. Josephson, *Adv. Phys.* **14**, 419 (1965).
  - [2] M. Sigrist and T. M. Rice, *J. Phys. Soc. Jpn.* **61**, 4283 (1992).
  - [3] D. A. Wollman *et al.*, *Phys. Rev. Lett.* **71**, 2134 (1993).
  - [4] R. Jin *et al.*, *Phys. Rev. B* **59**, 4433 (1999).
  - [5] M. Yamashiro, Y. Tanaka, and S. Kashiwaya, *J. Phys. Soc. Jpn.* **67**, 3364 (1998).
  - [6] C. Honerkamp and M. Sigrist, *Prog. Theor. Phys.* **100**, 53 (1998).
  - [7] S. Backhaus *et al.*, *Nature (London)* **392**, 687 (1998).
  - [8] A. Marchenkov *et al.*, *Phys. Rev. Lett.* **83**, 3860 (1999).
  - [9] O. Avenel, Y. Mukharsky, and E. Varoquaux, *Physica (Amsterdam)* **280B**, 130 (2000).
  - [10] S.-K. Yip, *Phys. Rev. Lett.* **83**, 3864 (1999).
  - [11] J. K. Viljas and E. V. Thuneberg, *Phys. Rev. Lett.* **83**, 3868 (1999).
  - [12] J. K. Viljas and E. V. Thuneberg, *Phys. Rev. B* **65**, 064530 (2002).
  - [13] A. Furusaki and M. Tsukada, *Solid State Commun.* **78**, 299 (1991).
  - [14] A. F. Andreev, *Zh. Eksp. Teor. Fiz.* **46**, 1823 (1964) [*Sov. Phys.* **19**, 1228 (1964)].
  - [15] S. Yip, *Phys. Rev. B* **32**, 2915 (1985).
  - [16] J. Kurkijärvi, *Phys. Rev. B* **38**, 11 184 (1988).
  - [17] Y. Tanaka and S. Kashiwaya, *Phys. Rev. B* **53**, R11 957 (1996).
  - [18] I. O. Kulik and A. N. Omel'yanchuk, *Fiz. Nizk. Temp.* **3**, 945 (1977) [*Sov. J. Low Temp. Phys.* **3**, 459 (1977)].
  - [19] A. Furusaki and M. Tsukada, *Phys. Rev. B* **43**, 10 164 (1991).
  - [20] D. J. Cousins *et al.*, *Phys. Rev. Lett.* **77**, 5245 (1996).
  - [21] A. J. Leggett and S. K. Yip, in *Helium Three*, edited by W. P. Halperin and L. P. Pitaevskii (North-Holland, Amsterdam, 1990), Chap. 8, p. 523.
  - [22] V. Ambegaokar, P. G. de Gennes, and D. Rainer, *Phys. Rev. A* **9**, 2676 (1974).
  - [23] R. Kaul and H. Kleinert, *J. Low Temp. Phys.* **38**, 539 (1980).
  - [24] S. Yip, *Phys. Rev. B* **35**, 8733 (1987).
  - [25] E. V. Thuneberg, *Physica (Amsterdam)* **178B**, 168 (1992).
  - [26] R. W. Simmonds *et al.*, *Phys. Rev. Lett.* **84**, 6062 (2000).
  - [27] E. V. Thuneberg, *Phys. Rev. B* **33**, 5124 (1986).
  - [28] Y. Asano, *Phys. Rev. B* **64**, 224 515 (2001).